A Calibration Process Focused on Predicting Both Energy Performance and Indoor Thermal Conditions

Saman Mostafavi[1], Benjamin Futrell[1], Robert W. Cox[1]
[1]UNC Charlotte, Charlotte, North Carolina

Abstract

This paper describes a new approach for calibrating whole-building energy models. In this case, we expose the building to a thermal-response test and observe its natural response to ambient conditions during unoccupied periods. This approach allows us to develop a calibrated model for the building structure using a set of conditions that more fully expose its complete dynamics. Subsequent calibration steps could be used to calibrate occupancy and system models as in Lam et al. (2014). The authors ultimately select parameters using the Bayesian calibration approach. The paper discusses both the rationale for the approach as well as the specific mechanism through which it is implemented. The superiority over whole-building energy calibration is demonstrated using a simulation study. Results from a real-world case study are also presented.

Introduction

Building energy models are intended to provide a reliable methodology for evaluating the energy-savings potential of various retrofit measures. To provide the highest degree of certainty, these models must be calibrated to determine appropriate values for uncertain model parameters (Yoon et al. (2003)). ASHRAE Guideline 14 provides a standard approach. First, audit data is used to develop a first-cut energy simulation (i.e. schedules, system nameplate information, etc.). Second, various uncertain model parameters are tuned by comparing whole-building energy predictions with measured values until any discrepancies fall within an acceptable tolerance. The standard practice is to reduce the coefficient of variation of the root-mean-square error (CVRMSE) to within 15 to 30 percent depending upon the frequency of the available energy data (Haberl et al. (2005)).

The second step in the simulation process, namely calibration, has typically followed a heuristic approach based on expert opinion (Pedrini et al. (2002)), but recent research has focused on numerical optimization methods (Taheri et al. (2013)), sensitivity analysis (Raftery et al. (2011)), and the adoption of Bayesian techniques (Riddle and Muehleisen (2014)). Traditional approaches focus on deterministically searching for a single solution that minimizes the difference between predicted and measured energy usage (Reddy (2006)). Parameters such as infiltration rates are generally tweaked until there is an acceptable fit, often ignoring other parameter combinations that may have a higher likelihood. In Heo et al. (2015), the authors demonstrated that Bayesian approaches can better match whole-building energy values while significantly lowering the uncertainty of the fit. This result, coupled with a general approach for applying Bayesian calibration, provides a powerful framework for better reducing model uncertainty.

Recent research has also examined the effectiveness of using additional data streams to help improve calibration. Lam et al. (2014), for instance, developed a multi-step procedure that uses real weather information, detailed sub-meters, and building automation system (BAS) data to improve the calibration process. The critical contributions of this work include methods for using empirical data to improve occupancy schedules and HVAC system and control parameters. The latter of these focuses upon examining actual zone temperature patterns. The underlying notion is that for predicted and measured energy values to match, one would expect that underlying zone temperatures should match as well since zone conditions drive HVAC energy consumption.

This paper more fully examines the notion that BAS data reflecting actual zone conditions can improve the calibration process. Specifically, we note that energy modelling is more appropriately viewed as a system-identification problem. In that context, we view the building envelope and its interior components as a dynamic system with various distributed mechanisms for both energy transfer and storage. As a dynamic system, we determine model parameters by examining the output signals in response to various input signals (Ljung (1999)). In the energy-modeling problem, this means

that we should determine model parameters by observing how the interior temperatures respond to various inputs such as weather and the heat gains from various interior loads. This approach has long been accepted in other engineering fields but has been challenging to implement with white-box energy models since only whole-building energy data has been traditionally available. Given the proliferation of automation systems and sub-meters, the authors believe it is appropriate to revisit the calibration problem. We have thus developed a procedure that decouples the calibration of envelope parameters (i.e. U-values, thermal mass, etc.) from the rest of the calibration process. In the demonstrated approach, we expose the building to what we term a thermal-response test in which we de-energize the HVAC system and allow the internal zone temperatures to exhibit their natural dynamic responses to exterior loading and internal heat sources. During this period, both weather and interior loads are monitored but the building is unoccupied. Note that we apply the Bayesian calibration technique to minimize the discrepancy between the measured and modeled zone temperatures. One could add more calibration layers that would adjust other parameters such as those for the HVAC system once the envelope parameters have been determined. This paper demonstrates that this process produces a model that more accurately reflects both whole-building energy consumption and interior temperatures.

The remaining sections of this paper describe the proposed calibration procedure. First, we discuss the underlying theory motivating the decision to perform calibration using zone temperature values. Subsequently, we describe the specific details of our approach, and we then compare our calibration method to state-of-the-art research focused on whole-building energy calibration (Heo et al. (2015)). This comparison is performed using the US Department of Energy stand-alone retail reference model DOE (2017). Finally, we present a real-world example using a retail bank branch located in Miami, Florida. Using our approach, we were able to decouple the independent impacts of various envelope and system measures. The paper concludes with a discussion on next steps.

Motivation

Whole-building simulation models represent the combined effects of the thermal behavior of the structure and its loads, the air-conditioning system, and the central plant. The zone-level model takes as input the building description, weather, and internal heat gains, and it calculates zone air temperatures and sensible loads. These are then used to determine air-conditioning system performance. At the zone level, the model balances all of the energy flows in each zone and involves the solution of a set of energy-balance equations for the zone air and the interior and exterior surfaces of each wall, roof, and floor. These equations are combined with others that represent transient conduction heat transfer through the walls and roof (McQuiston et al. (2005)).

The heat-transfer process within each zone is most properly described using appropriate partial differential equations. Various lumped-element simplifications have been developed over time to describe the dynamics of the interactions between the walls, floor, ceiling, internal contents, and adjacent zones. Most white-box energy models begin with a simplified heat balance for the zone air. Using the definitions provided in Table 1, we formulate this as

$$C_z \frac{dT_z}{dt} = \sum_{i=1}^{N_{sl}} \dot{Q}_i + \sum_{i=1}^{N_{surfaces}} h_i A_i (T_{si} - T_z) + \sum_{i=1}^{N_{zones}} \dot{m}_i C_p (T_{zi} - T_z) + \dot{Q}_{inf} + \dot{Q}_{sys} \quad (1)$$

Recall that this dynamic model captures only a portion of the process, as heat conducts slowly through walls and radiant energy becomes absorbed by floors, interior walls, and furniture only to be slowly transferred into the air mass by convection (McQuiston et al. (2005)). To capture these effects using a white-box model requires the use of many parameters, and the modeler typically chooses initial values for these based on construction documents and some combination of experience and sound engineering judgement (Reddy (2006)). Because they contain many interconnected parameters, white-box energy models do not fit naturally into the framework of system identification. Instead, one adjusts the model parameters in a reasonable manner using either intuition or some form of sensitivity analysis or numerical optimization. Models are deemed to be calibrated when the predicted whole-building energy consumption matches its actual value within some tolerance, typically on a monthly basis since monthly values tend to be the most readily available.

Figure 1 demonstrates potential problems with the traditional calibration approach. This figure shows both the measured and modeled temperatures in one zone of the retail bank discussed in the experimental section of this paper. Note that the HVAC system maintains the system at approximately 72°F during occupied hours. Once the bank closes each evening, the temperature is setback to enable the system to turn off and hence reduce its energy consumption. Note that the predicted zone temperature reaches the setpoint several hours before the actual zone temperature does the same. This

Table 1: Definitions for parameters used in Eq. 1. (DOE (2016))

Parameter	Description
Q_i	i^{th} internal convective load
C_z	zone air capacitance ($\rho_{air} C_p C_T$)
ρ_{air}	zone air density
C_p	zone air specific heat
C_T	sensible heat capacity multiplier
$\dot{Q}_{inf}$	heat transfer due to infiltration
$\dot{Q}_{sys}$	air system output
T_z	zone temperature
$N_{surfaces}$	number of zone surfaces
N_{zones}	number of adjacent zones
N_{sl}	number of convective loads
$h_i A_i (T_{si} - T_z)$	zone convective heat transfer with i^{th} surface
$m_i C_p (T_{zi} - T_z)$	interzone heat transfer with i^{th} zone
m_i	mass flow rate into i^{th} zone
h_i	heat transfer coeff. from i^{th} surf.
T_{si}	temperature of the i^{th} surface
T_{zi}	temp. of the i^{th} adjacent zone
A_i	area of the i^{th} surf.

behavior indicates that several critical parameters must been inaccurately determined. In this case, however, Figure 2 shows that the predicted and actual monthly energy values closely match, with an overall CVRMSE of 10.1%, which is well within ASHRAE guidelines.

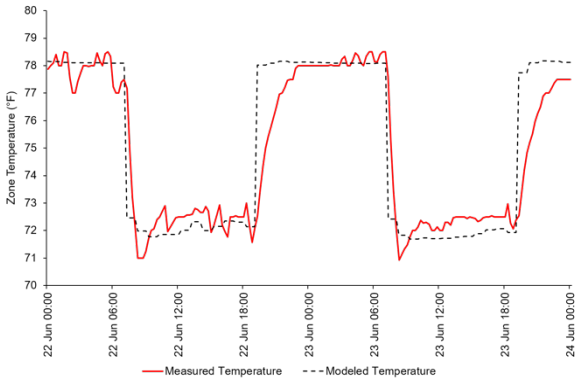

Figure 1: Measured and modeled zone temperatures in Zone 3 of our test facility. The model was produced by the air-conditioning system manufacturer.

Figure 1 highlights the inherent problems associated with ignoring the underlying dynamics of the building model, and it suggests the alternative approach proposed here. If we consider the model to be linear and time-invariant (LTI), then it can be fully characterized by its impulse response or some equivalent measure

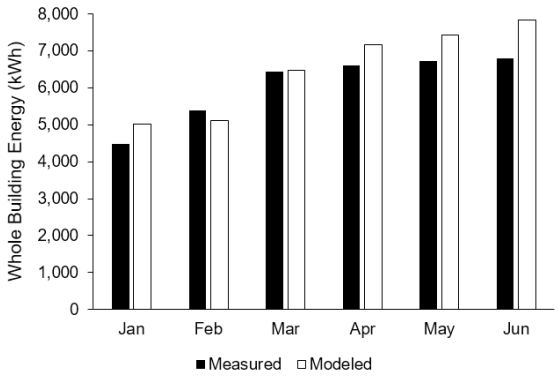

Figure 2: Measured and modeled monthly energy for the same test facility considered in Fig. 1.

such as its step or frequency response (Ljung (1999)). Although the system is not LTI, this simplification is more than reasonable and has been demonstrated by numerous other authors (Li and Wen (2014)). We know that the true parameters should be learned by exposing the system to an input that exercises the underlying dynamics. If we rely largely on steady-state conditions during which the HVAC system is maintaining a constant temperature, the dynamics will be masked and we will greatly increase the likelihood of finding inappropriate parameter values. We thus consider our model to be calibrated when the predicted zone-temperature profiles match their actual values during conditions in which the HVAC system is de-energized and the true dynamics are exposed. Since white-box energy models are so highly parametrized, we know that this method still cannot guarantee that we find the exact set of parameter values. It can, however, ensure that the model accurately predicts the true cooling load profile within the space. Given that one typically uses an energy model to determine the impact of various energy-saving technologies such as improved insulation or windows, then the determination of appropriate cooling-load patterns is critical.

Approach

Previous sections have described the basic procedure used to calibrate the envelope parameters. In practice, we de-energize the space-conditioning systems and observe the building's response to its natural loading conditions. We perform this test during an unoccupied period, and we record both weather and space temperatures throughout. Sub-meters are used to track the actual internal heat gains.

Our calibration procedure uses Bayesian inference to determine a set of parameter values that could have generated the observed temperature patterns given the observed weather and internal heat gains. We are thus

utilizing a relatively new technique (i.e. Bayesian calibration) in a manner that is itself a departure from orthodoxy (i.e. calibrating using a measured thermal response rather than whole-building energy). In the end, the approach has continually produced models with low energy errors and appropriate thermal responses. The impact of this decision to calibrate using temperature profiles rather than whole-building energy is explored more deeply in the next section. The remainder of this section describes the details of this process.

Bayesian Calibration

Bayesian calibration, which has recently attracted much attention in the literature (Riddle and Muehleisen (2014); Heo et al. (2015)) uses Bayesian inference to estimate a set of likely parameter distributions, rather than a single set of parameters that could be one of many that produce similar temperature profiles. Given these parameter distributions, the resulting model thus computes a set of possible outcomes, each having its own associated confidence value, rather than a single expected output. In this framework, each parameter has a prior probability density function that expresses the modeler's prior beliefs in the true parameter values. In this context, the term probability refers to a numerical estimate of one's degree of belief in the hypothesized value. With each parameter grouped in a composite vector θ, we denote the prior densities as $p(\theta)$. As calibration iteratively proceeds, these prior distributions are updated using measured data. In this case, the measurements are zone temperatures. For each calibration experiment, we compute a model performacne metric D expressing the goodness-of-fit between the actual zone temperature profiles and their predicted profiles. We then compute a likelihood $p(D|\theta)$ expressing the probability that a given parameter set yielded the measured temperatures. During the calibration process, we perform a multitude of simulations, and after each we compute a new value D as well as the corresponding posterior distribution $p(\theta|D)$. This distribution is determined from Bayes' Theorem (Gelman et al. (2014)), i.e.

$$p(\theta|D) \propto p(\theta) \times p(D|\theta). \tag{2}$$

The process proceeds until the modeler deems the posterior distributions to be appropriate. Under the central limit theorem, one would expect the process to proceed until the distributions become normal (Gelman et al. (2014)). This posterior distribution can be then used as the prior distribution for the subsequent calibration.

Figure 3 shows how we implement the calibration process. This resembles a Metropolis-Hastings algorithm (Gelman et al. (2014).). We begin with a randomly chosen parameter set θ'. We then run the simulation

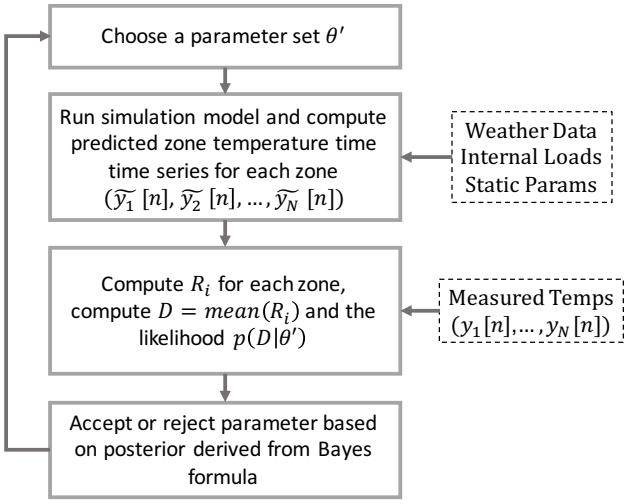

Figure 3: The calibration process.

model using measured weather and load patterns, and we produce a set of outputs, namely the N zone temperatures. For the i^{th} zone we denote the predicted zone temperatures as a time series $\tilde{y}_i[n]$, where the index n denotes the time. The data is sampled at one-hour intervals. Once the predictions are calculated, we use the measured values to compute the goodness-of-fit metric D. This is a two-step process. First, we calculate the index of agreement R_i, which we define as

$$R_i = 1 - \frac{\sum_{n=1}^{M} \left(\frac{\tilde{y}_i[n] - y_i[n]}{\tilde{y}_i[n]} \right)^2}{\sum_{n=1}^{M} \left(\frac{|\tilde{y}_i[n] - \bar{y}_i| + |y_i[n] - \bar{y}_i|}{\bar{y}_i} \right)^2}, \tag{3}$$

where M is the total number of samples in each time series and $\bar{y}_i$ is the mean of the observed time series $y_i[n]$. This index has a value between 0 and 1 with values closer to 1 indicating stronger correlations between the two time series. We then compute D as the average of R over all zones,i.e.

$$D = \frac{1}{N} \sum_{i=1}^{N} R_i. \tag{4}$$

The likelihood function $p(D|\theta')$ is the probability density of the model performance metric D given the selected parameter values θ'. In this case, we model the observations given the parameters as:

$$p(D|\theta') = e^{-\pi(D-1)^2}, \tag{5}$$

which is a normal distribution with mean 1 and variance $\frac{1}{2\pi}$. The reason behind choosing a bell curve for the likelihood pdf lies behind the logic that a worse model performance should be an indication of bad parameter

selection and therefor less likely parameters. The normal model provides a good decay rate for this purpose. Here, based on our defined performance metric, if D has the value 1, the parameters have a likelihood of 1. As the value D goes toward zero so does the probability $p(D|\theta')$. Further examples of likelihood function selection are available in Gelman et al. (2014). Once we compute the likelihood function, we compute the posterior distribution $p(\theta|D)$ using Bayes' Theorem. If the posterior is improved in comparison to the posterior of a previous candidate, we store the candidate parameter θ'. Otherwise, we either store the new candidate or store the previous one in a random manner (this resembles a random walk process).

As we proceed from one simulation to the next, we select a new candidate parameter set θ' using a normal jumping distribution J. This would result in a final marginal posterior distributions with a normal appearance (Gelman et al. (2014)). Therefor the simulation process should ideally continue until the posterior takes a normal shape. Denoting each simulation as having an index t, then we can say that we select θ^t from adding a normal jump to θ^{t-1}. The specifics of the Metropolis-Hastings algorithm are beyond the scope of this paper, and the interested reader is directed to Gelman et al. (2014).

It should be noted that we begin our simulations by assuming uniform prior distributions. Others have assumed different distributions, including triangular shapes (Heo et al. (2015)). We have found that both triangular and uniform distributions both lead to appropriate convergence and thus we have made the decision to use the simple uniform distribution.

Simulation Study: Demonstrating the Importance of Zone Temperatures

To explore the impact of calibrating using zone temperatures, the authors considered the US Department of Energy stand-alone retail reference model (DOE (2017)). Figure 4 shows a simple rendering of this building. The authors performed calibration using two approaches:

1. **Method 1 - Whole-building energy methodology**: Bayesian calibration is applied to the monthly whole-building energy value as in Heo et al. (2015)
2. **Method 2 - Zone-temperature methodology**: Bayesian calibration is applied to the uncontrolled zone-temperature profiles as proposed in this paper.

Before beginning the calibration process, the authors used their judgment to determine a set of parameters likely to have a strong impact on the envelope thermal model. Table 2 lists these parameters and their initial values. Each was assumed to be uniformly distributed over a range extending from ±50% of this initial value. Before calibrating, we first performed a sensitivity analysis intended to determine the most influential parameters. To perform the analysis, we computed the so-called Spearman correlation coefficient (SCC) for each parameter using the approach described in Groen et al. (2016). The higher this value, the more influential the impact of the parameter on the model. More complete details are presented in Groen et al. (2016). The parameters presented in Table 2 are ranked from most influential (top) to least influential (bottom). We ultimately performed our calibrations using the five most influential parameters. Explanations for the units of each can be found in the EnergyPlus Engineering Reference (DOE (2016)). Infiltration, for instance, is defined as the volumetric flow rate per exterior surface area; hence the units $(m^3/s)/m^2$ (DOE (2016)).

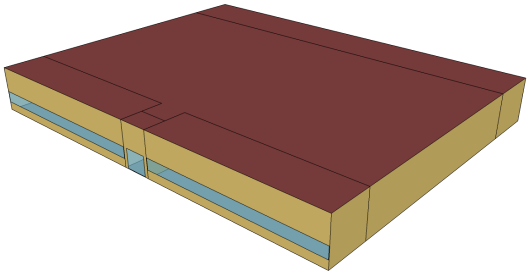

Figure 4: Simple rendering of the DOE stand-alone retail reference model.

Table 2: Parameters considered during the sensitivity analysis. Values are ranked based on their Spearman correlation coefficients (Groen et al. (2016)), with the most influential parameter placed on top.

Model Parameter	**True Value**
Zone 1 infil. $((m^3/s)/m^2)$	0.0003
Zone 1 Internal Mass (m^2)	3201
Zone 2 Internal Mass (m^2)	760
Zone 4 Internal Mass (m^2)	301.62
Zone 3 Internal Mass (m^2)	301.62
Ground Reflectance	0.2
Roof Cond. (W/(m°K))	0.049
Ufactor (W/(m^2°K))	6.92
SHGC	0.25
Wall Cond. (W/(m°K))	1.31
Floor Cond. (W/(m°K))	1.31
Zone 2 infil. $((m^3/s)/m^2)$	1
Zone 5 Internal Mass (m^2)	24

Ultimately, 30,000 simulations were performed using each of the two calibration procedures. Method 1 (the whole-building energy approach) yielded an annual en-

ergy CVRMSE of 0.97%, and method 2 (the zone temperature approach) yielded an annual energy CVRMSE of 0.67%. Both are thus well within accepted guidelines. Figure 5, however, shows that the two methods yielded vastly different posterior distributions for the three most influential parameters, namely Zone 1 infiltration rate, Zone 1 internal mass, and Zone 2 internal mass. The top row (a, b, and c) shows the results obtained using the whole-building energy methodology, and the bottom row (d, e, and f) shows the results obtained using the zone-temperature methodology. The true parameter values are indicated using red dashed lines. Note that only in the case of the zone-temperature methodology do the expected values of each parameter converge near to their true values. In the case of Zone 1 infiltration, for instance, the expected value is approximately a factor of 3 below the true value. Such errors can be significant if one seeks to accurately reflect the contributions of various retrofit measures.

To demonstrate the impact on the temperature profiles, we computed the residuals $y_i[n] - \tilde{y}_i[n]$. Figure 6 shows the results for Zone 1 over one month. The top image shows the residuals obtained using the whole-building energy methodology; the bottom image shows the residuals obtained using the zone-temperature methodology. If the model is well calibrated, one would expect these residuals to be normally distributed around 0. In the case of the whole-building energy methodology, the residuals are centered around a bias of 0.0802°C and possess a skewed distribution having a much larger variance. These results demonstrate that the more accurate parameter estimates obtained using the proposed zone-temperature approach produce a more accurate prediction of the cooling load.

Experimental Results

The authors also tested the proposed approach in a 325.16m^2 retail bank in Miami, Florida. The goal was to individually evaluate the impact of various technology choices, including electrochromic glass, insulated concrete forms, and variable refrigerant flow (VRF) HVAC. Figure 6 shows a simple rendering of the building and its three thermal zones, which include an open-plan office and lobby, a teller line, individual offices, and several shared spaces (i.e. break room, restrooms). One might initially suggest that such small facilities do not merit such detailed analysis, but the development of a thorough model is driven by the fact that the proposed design is a prototype for a large corporation that develops dozens of new locations each year and retrofits dozens more. A thorough model can thus be used to guide the investment in appropriate technologies for various climate zones and building locations.

To measure the thermal response, we de-energized the VRF system and its corresponding dedicated outside air system (DOAS) beginning approximately one hour after business concluded on several Saturday afternoons. The building remained unconditioned until early the following Monday morning. The bank has an extensive BAS that records the hourly energy usage for each electrical circuit; zone temperatures are recorded on change. These measurements as well as weather data are recorded throughout the test. Dry bulb temperature, wind speed, relative humidity, and irradiance are obtained from internet resources. These measurements are used as inputs to the energy model, which was developed in EnergyPlus. Figure 8 shows the measured thermal response in each zone during the training weekend in August 2015. Each plot also shows the results of the initial, uncalibrated model developed based on the construction documents.

Calibration begins by first selecting the most influential parameters. Table 3 lists the seven chosen parameters and the range of values selected for the corresponding uniform prior distribution function. Note that since the building utilizes electrochromic glass, the solar heat gain coefficient (SHGC) changes throughout the day in accordance with the amount of solar radiation incident on a given facade. Our model treats the windows on each facade differently, and it changes the SHGC appropriately as the solar radiation varies. The SHGC parameter listed in Table 3 is thus the value used when a given window is tinted. The clear condition value is treated as fixed, and the model selects the appropriate value using measured control signals.

Table 3: The most influential structural parameters in the prototype retail bank model.

Structural Parameter	**Range**
SHGC	0.01 - 0.135
Roof Insulation Cond. (W/(m°K))	0.02 - 0.1
Floor Cond. (W/(m°K))	1 - 4
Infil. Rate ((m^3/s)/m^2)	0.0001 - 0.0004
Zone 1 Internal Mass (m^2)	80 - 1000
Zone 2 Internal Mass (m^2)	80 - 1000
Zone 3 Internal Mass (m^2)	80 - 1400

The calibration process begins using samples drawn from the uniform distributions outlined in Table 3. Subsequent simulations drive to the posterior distributions as described previously. In our current approach, we perform 30,000 model iterations, and derive posterior distributions such as the ones shown in Figure 9 for the thermal masses in Zones 2 and 3, respectively. Note that these final posterior distributions fit closely to normal distributions, suggesting that the calibration process is likely converging to true values for these pa-

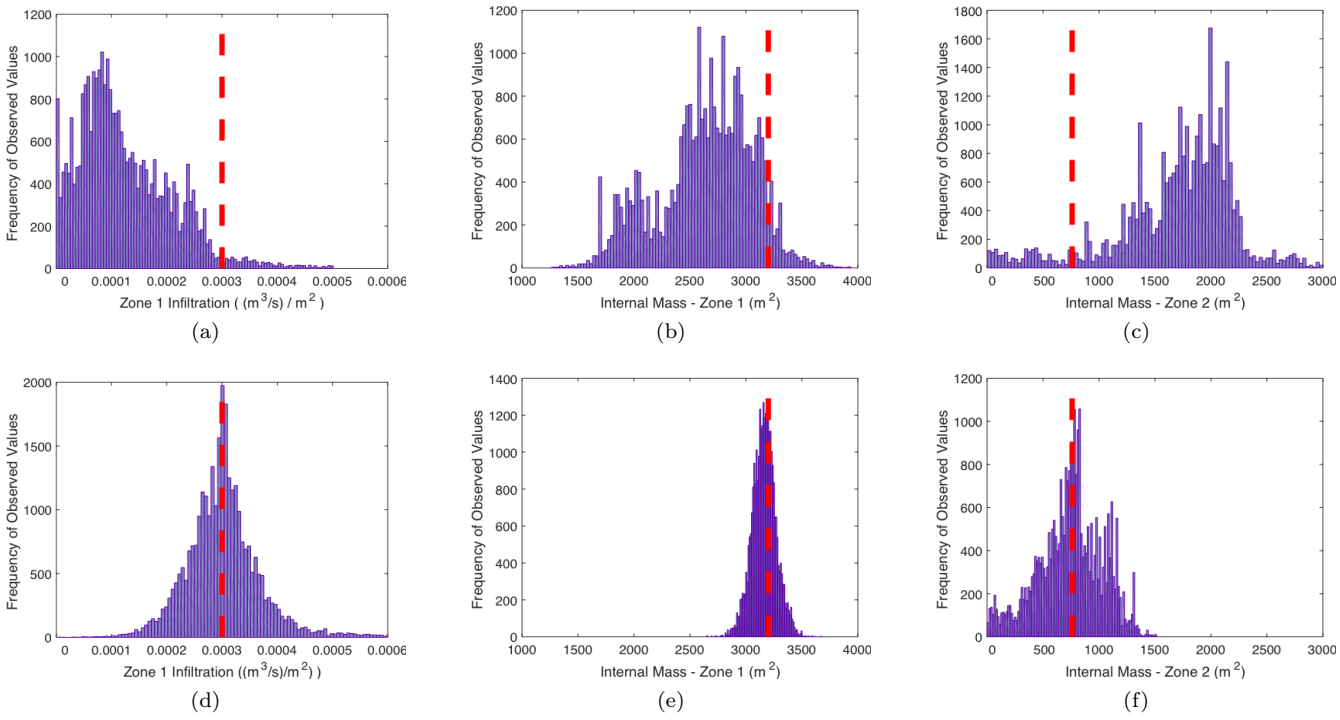

Figure 5: Posterior distributions for the three most significant parameter values. The top row shows results from Method 1 (Whole-building methodology); the bottom row shows results from Method 2 (zone-temperature methodology). (a) and (d) show distributions for Zone 1 infiltration; (b) and (e) show distributions for Zone 1 internal mass; and (c) and (f) show distributions for Zone 2 internal mass. The true parameter values are indicated with a red dashed line. Note that the expected values of the distributions found using Method 2 are much closer to the true values.

rameters. To evaluate the model output, we select one hundred random samples from the learned distributions and compute the expected zone temperature time series for each one. A corresponding confidence interval is then calculated. Figure 10 shows the measured zone temperature as well as the upper and lower 97% confidence intervals produced for Zone 2 using the 100 parameter sets. The top graph in that figure shows the modeled and actual results for Zone 2 over the training weekend. Note the visual improvement of this fit over that shown in Figure 8. For validation purposes, the same parameter sets were used with thermal-response data measured during two different validation intervals. Figure 10b shows the measured and predicted results for Zone 2 using data collected in mid-February when ambient conditions were quite different. Note that the model outputs in that Figure were computed using the same distributions determined from the August training interval. Again, note the visual appeal of the fit despite the different ambient conditions.

Given that temperature profiles are not typically used to calibrate energy models, it is only sensible to compare actual energy performance. Figure 11 shows the resulting monthly whole-building energy computed using both our model and the VRF manufacturer's model discussed in the "Motivation" section. Note that both models produce nearly identical energy performance, and that both are within acceptable bounds according to ASHRAE Guideline 14 (our calibrated model has CVRMSE = 10.5% and the manufacturers heuristically calibrated model has CVRMSE = 10.1%). Given that both show acceptable energy performance, the results merit closer investigation. To frame that discussion, compare the conditioned temperature profile shown in Figure 12 to that determined from the manufacturers model as presented in Figure 1. Note that our calibrated model better predicts the trajectory of the temperature rise during the evening setback period. Given that the building envelope and interior elements were calibrated in the absence of space conditioning, our model more accurately predicts the impact of exterior and interior heat gains on the actual cooling loads. A careful investigation found that the manufacturer's model did not match the actual sequence of operations. It assumed a more efficient VRF system and a higher cooling load. The manufacturer has recently noted this

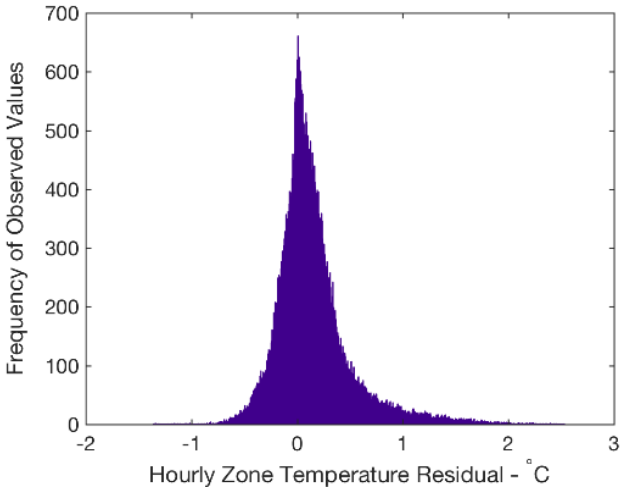

(a)

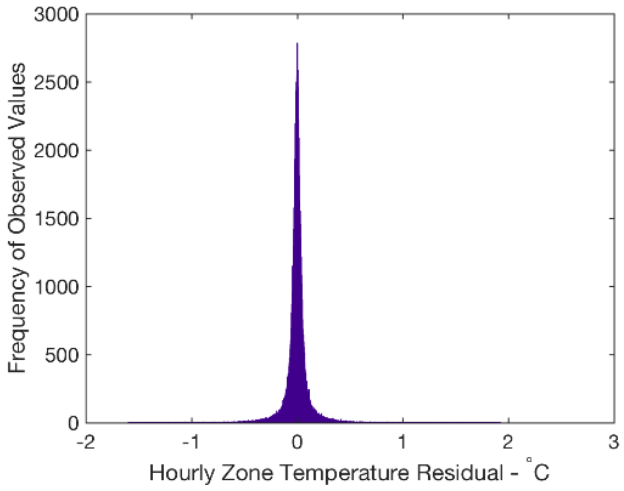

(b)

Figure 6: Hourly zone temperature residuals for zone 1 over one month. (a) Residuals from Method 1 (whole-building energy methodology) and (b) residuals from Method 2 (zone-temperature methodology).

fact and the controls are in the process of being upgraded.

Note that we can further reduce errors in our whole-building energy prediction. Much of the remaining error arises from a fan that occasionally cycles to transfer cool air from the lobby to an ATM closet. The high flow rate of this fan has been found to impact the cooling effectiveness in Zones 1 and 2. The authors note that accounting for this effect will likely further reduce errors.

The transfer fan anecdote illustrates an important rationale for our proposed approach. When the transfer fan is in operation, the resulting loss of delivered

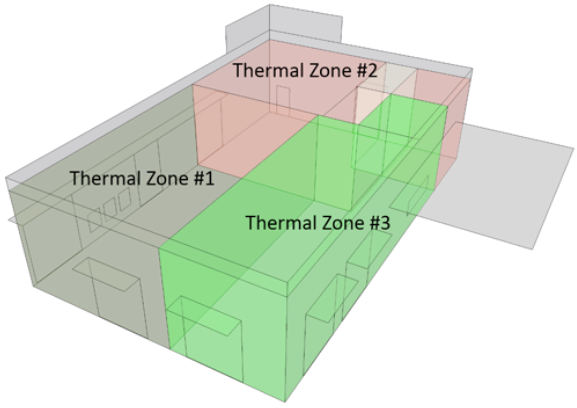

Figure 7: Simple rendering of the prototype bank. The basic design is similar to that used at all of the corporations US locations.

capacity in Zones 1 and 2 drives the zone temperatures slightly upward. If using an effective set point adjustment as proposed in Lam et al. (2014), the authors would have simply adjusted the set points in their model to account for this effect without knowing the exact cause. Using our approach, we know that the envelope is better captured, and thus we have a more direct framework to be able to determine the root cause of the need for effective set point changes. The authors note that the general framework of Lam et al. (2014) is still incredibly powerful, and that our work is essentially a modification that would further improve that approach. Our envelope calibration should thus be followed by similar system-level calibrations as in Lam et al. (2014).

Conclusions & Future Work

This paper presents a brief introduction to the proposed approach. Ultimately, two innovations are under investigation. The first is the concept of decoupling the building envelope and its interior mass from the overall whole-building calibration process. In addition, however, this paper presents one of the first real-world applications of Bayesian calibration. The work highlights both the useful nature of the proposed decoupling as well the inherent power of the Bayesian framework. The findings suggest that the combination of the proposed approach with Bayesian calibration could be used to further strengthen a powerful framework such as the one proposed in Lam et al. (2014).

It should be noted that the computational effort associated with this approach is not too great. $30,000$ model iterations can be performed with our models using modern, off-the-shelf desktop PCs in approximately 8 hours. More advanced computers could greatly reduce this time. Additionally, we could consider stop-

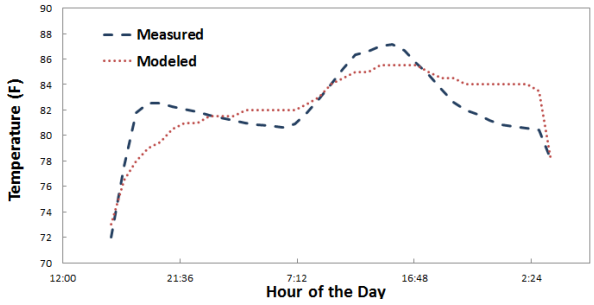

(a)

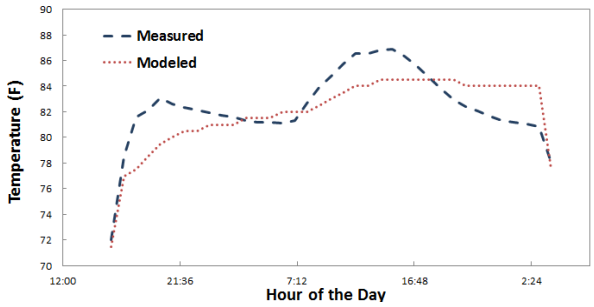

(b)

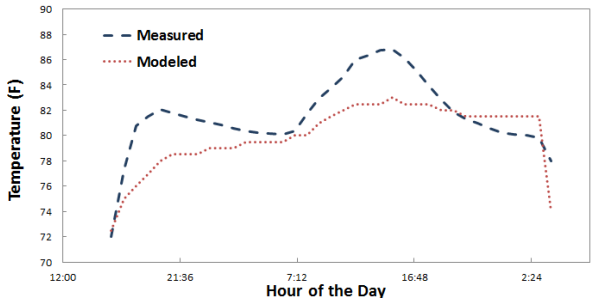

(c)

Figure 8: Un-Calibrated model performance during Aug 2nd for (a) zone one (b) zone two, and (c) zone three

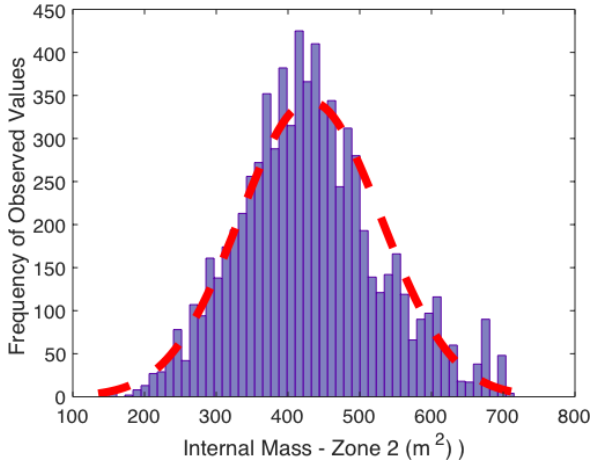

(a)

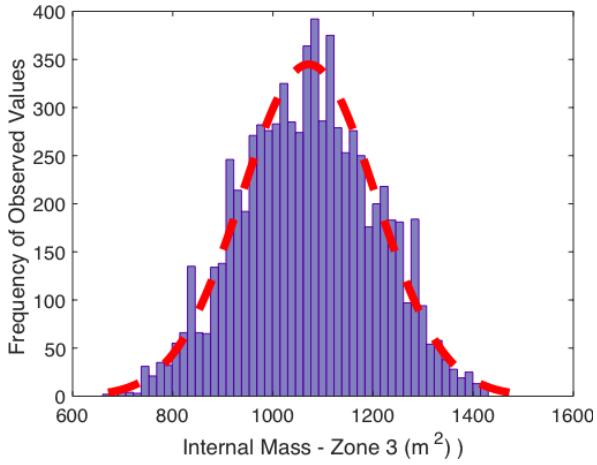

(b)

Figure 9: Posterior distributions for key parameters in the experimental model. (a) Internal mass in Zone 2 (b) Internal mass in Zone 3.

ping criteria, since 30,000 iterations may not be necessary for the parameters to converge. This issue requires further investigation. The goal here has simply been to demonstrate the approach. Future studies will examine the implementation details.

Acknowledgement

This material is based upon work supported by the National Science Foundation under grant no. IIP-1161031.

References

DOE (2016). EnergyPlus Engineering Reference. The Reference to EnergyPlus Calculations.

DOE (2017). Reference buildings by building type: Stand-alone retail. https://energy.gov/eere/downloads/reference-buildings-building-type-stand-alone-retail.

Gelman, A., J. B. Carlin, H. S. Stern, and D. B. Rubin (2014). *Bayesian data analysis*, Volume 2. Boca Raton: Chapman & Hall/CRC.

Groen, E. A., E. A. Bokkers, R. Heijungs, and I. J. de Boer (2016). Methods for global sensitivity analysis in life cycle assessment. *The International Journal of Life Cycle Assessment*, 1–13.

Haberl, J. S., D. Claridge, and C. Culp (2005). ASHRAE's guideline 14-2002 for measurement of energy and demand savings: How to determine what was really saved by the retrofit. In *Proc. of the 5th Int. Conf. for Enhanced Building Operations*.

Heo, Y., D. J. Graziano, L. Guzowski, and R. T. Muehleisen (2015). Evaluation of calibration efficacy under different levels of uncertainty. *Journal of Building Performance Simulation 8*(3), 135–144.

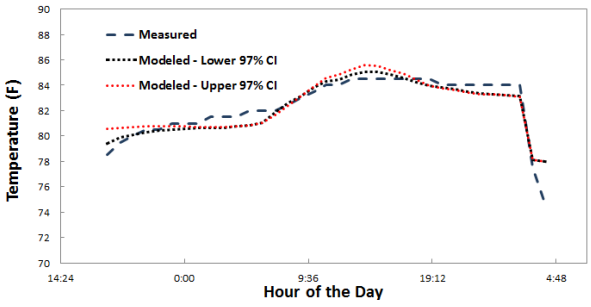

(a)

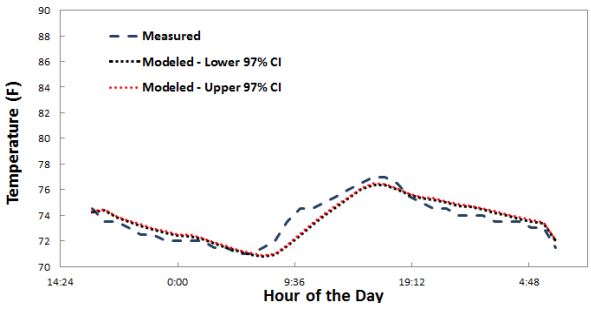

(b)

Figure 10: Temperatures in Zone 2 during thermal response testing (a) During the August training period and (b) during the February validation period.

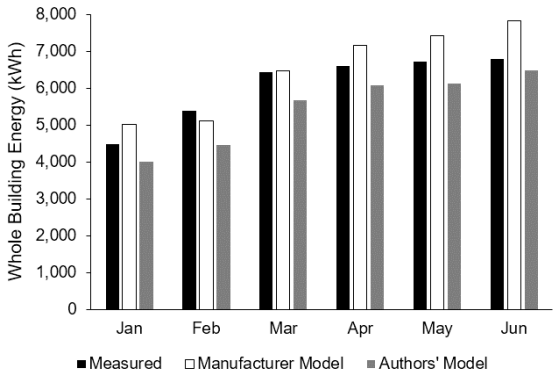

Figure 11: Comparison between the measured monthly energy and the predicted monthly energy computed using both our calibrated model and the manufacturer's heuristically calibrated model.

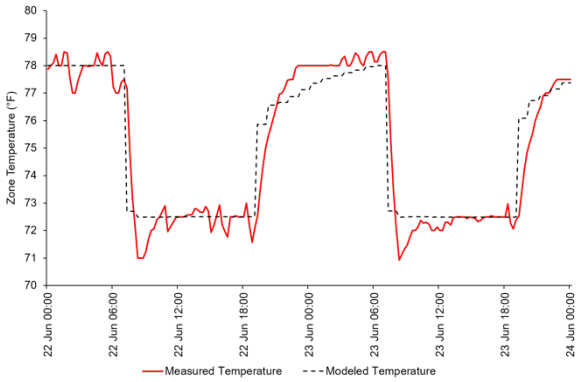

Figure 12: Temperature plots for Zone 3 using our calibrated model parameters. This was developed using the same conditions as in Figure 1.

Lam, K. P., J. Zhao, B. E. Ydstie, J. Wirick, M. Qi, and J. Park (2014). An EnergyPlus whole building energy model calibration method for office buildings using occupant behavior data mining and empirical data. In *Proc. ASHRAE IBPSA-USA Building Simulation Conf.*, pp. 160–167.

Li, X. and J. Wen (2014). Review of building energy modeling for control and operation. *Renewable and Sustainable Energy Reviews 37*, 517–537.

Ljung, L. (1999). *System Identification: Theory for the User* (2 ed.). Prentice Hall.

McQuiston, F., J. Parker, and J. Spitler (2005). *Heating, Ventilating, and Air Conditioning: Analysis and Design* (6 ed.). New York: John Wiley and Sons., Inc.

Pedrini, A., F. Westphal, F. Simon, and R. L. Roberto (2002). A methodology for building energy modelling and calibration in warm climates. *Building and Environment 37*(8), 903–912.

Raftery, P., M. Keane, and J. ODonnell (2011). Calibrating whole building energy models: An evidence-based methodology. *Energy and Buildings 43*(9), 2356–2364.

Reddy, T. A. (2006). Literature review on calibration of building energy simulation programs: Uses, problems, procedures, uncertainty, and tools. *ASHRAE Transactions 112*(1), 226–240.

Riddle, M. and R. T. Muehleisen (2014). A guide to bayesian calibration of building energy models. In *Proc. Building Simulation Conf.*

Taheri, M., F. Tahmasebi, and A. Mahdavi (2013). A case study of optimization-aided thermal building performance simulation calibration. In *Proc. 13th Int. Conf. of the International Building Performance Simulation Association.*

Yoon, J., E. Lee, and D.E.Claridge (2003). Calibration procedure for energy performance simulation of a commercial building. *Journal of Solar Energy Engineering 125*(3), 251–257.